Bone Reports 17 (2022) 101615

Contents lists available at ScienceDirect

Bone Reports

journal homepage: www.elsevier.com/locate/bonr

# Cortical bone relationships are maintained regardless of sex and diet in a large population of LGXSM advanced intercross mice

Nicole Migotsky [a,b,*], Michael D. Brodt [a], James M. Cheverud [c], Matthew J. Silva [a,b]

[a] Department of Orthopaedic Surgery and Musculoskeletal Research Center, Washington University in St. Louis, 660 S. Euclid, St. Louis, MO 63110, United States of America
[b] Department of Biomedical Engineering, Washington University in St. Louis, 1 Brookings Drive, St. Louis, MO 63130, United States of America
[c] Department of Biology, Loyola University, 1032 W. Sheridan Road, Chicago, IL 60660, United States of America

ARTICLE INFO

*Keywords:*
Biomechanics
Micro-computed tomography
Dimensional reduction
Morphology
Mechanical properties
Material properties

ABSTRACT

*Introduction:* Knowledge of bone structure-function relationships in mice has been based on relatively small sample sets that limit generalizability. We sought to investigate structure-function relationships of long bones from a large population of genetically diverse mice. Therefore, we analyzed previously published data from the femur and radius of male and female mice from the F34 generation of the Large-by-Small advanced intercross line (LGXSM AI), which have over a two-fold continuous spread of bone and body sizes (Silva et al. 2019 JBMR).
*Methods:* Morphological traits, mechanical properties, and estimated material properties were collected from the femur and radius from 1113 LGXSM AI adult mice (avg. age 25 wks). Males and females fed a low-fat or high-fat diet were evaluated to increase population variation. The data were analyzed using principal component analysis (PCA), Pearson's correlation, and multivariate linear regression.
*Results:* Using PCA groupings and hierarchical clustering, we identified a reduced set of traits that span the population variation and are relatively independent of each other. These include three morphometry parameters (cortical area, medullary area, and length), two mechanical properties (ultimate force and post-yield displacement), and one material property (ultimate stress). When comparing traits of the femur to the radius, morphological traits are moderately well correlated ($r^2$: 0.18–0.44) and independent of sex and diet. However, mechanical and material properties are weakly correlated or uncorrelated between the long bones. Ultimate force can be predicted from morphology with moderate accuracy for both long bones independent of variations due to genetics, sex, or diet; however, predictions miss up to 50 % of the variation in the population. Estimated material properties in the femur are moderately to strongly correlated with bone size parameters, while these correlations are very weak in the radius.
*Discussion:* Our results indicate that variation in cortical bone phenotype in the F34 LGXSM AI mouse population can be adequately described by a reduced set of bone traits. These traits include cortical area, medullary area, bone length, ultimate force, post-yield displacement, and ultimate stress. The weak correlation of mechanical and material properties between the femur and radius indicates that the results from routine three-point bending tests of one long bone (e.g., femur) may not be generalizable to another long bone (e.g., radius). Additionally, these properties could not be fully predicted from bone morphology alone, confirming the importance of mechanical testing. Finally, material properties of the femur estimated based on beam theory equations showed a strong dependence on geometry that was not seen in the radius, suggesting that differences in femur size within a study may confound interpretation of estimated material properties.

## 1. Introduction

Investigating the mechanical strength of long bones is a well-established concept in biology and engineering (Burstein and Frankel, 1971; Pelker et al., 1983). Turner and Burr laid a foundation for biomechanical testing of rodent bones by describing techniques and

* Corresponding author at: Department of Orthopaedic Surgery and Musculoskeletal Research Center, Washington University in St. Louis, 660 S. Euclid, St. Louis, MO 63110, United States of America.
*E-mail address:* n.migotsky@wustl.edu (N. Migotsky).

https://doi.org/10.1016/j.bonr.2022.101615
Received 17 May 2022; Received in revised form 6 July 2022; Accepted 25 August 2022
Available online 26 August 2022

defining terminology (Turner and Burr, 1993). These methods have become a staple in phenotyping musculoskeletal mouse models, allowing researchers to identify quantitative trait loci (QTL) (Lang et al., 2005), analyze gene functions (Bonadio et al., 1993; Mikić et al., 1995; Mikić et al., 1996), assess responses to pharmacological interventions (Brent et al., 2021) and alterations in mechanical loading (Holguin et al., n.d.; Berman et al., 2015), and quantify changes with growth and aging (Brodt et al., 1999; Jepsen et al., 2015).

Knowing the strength of bones alongside morphology allows the investigation of structure-function relationships. It has been shown that bone material can redistribute, especially if quality is altered, to preserve adequate whole-bone (structural) strength (Bonadio et al., 1993; Mikić et al., 1995; Mikić et al., 1996; Lanyon et al., 1982; Goodship et al., 1979). Jepsen et al. identified three adaptations to meet the needs of the skeletal loading environment: changing the amount of bone, the distribution of bone, or the quality of bone (Jepsen et al., 2003a). For example, in a mouse model of osteogenesis imperfecta (OI), mutant mice compensate for deficient collagen production by developing larger bones which leads to an increase in whole-bone strength (Bonadio et al., 1993). Conversely, mice with BMP-5 deficiency, which have smaller body and muscle mass, develop smaller, weaker bones, while maintaining bone composition and material properties consistent with lower mechanical demands (Mikić et al., 1995; Mikić et al., 1996). These examples highlight the importance of examining mechanical and morphological properties of bones together (Jepsen et al., 2015).

While mechanical testing of mouse bones has provided insights into bone structure-function, there remain some limitations. First, many studies use only one strain of mouse (Brodt et al., 1999; Gardinier et al., 2016), and those that use more than one typically use discrete inbred strains (Jepsen et al., 2001; Jepsen et al., 2003b). This can lead to groupings or clusters of data at two extremes instead of a continuous distribution of values, making correlations between traits difficult to assess (Voide et al., 2008). Second, despite knowing there are differences in regulation of bone strength and morphology between females and males (Cole and van der Meulen, 2011; Turner et al., 2003), many studies only evaluate one sex (Berman et al., 2015; Brodt et al., 1999). Third, sample sizes are typically tens of mice (Jepsen et al., 2003a; Jepsen et al., 2001). Fourth, most studies only evaluate a single bone per mouse. Collectively, these drawbacks limit the opportunity for generalizable conclusions. Lang et al. addressed these limitations by testing mice from the F2 generation of C57 x DBA mice, using males and females, a sample size of 200 per sex, and evaluating both the tibia and femur (Lang et al., 2005). However, the focus of that study was to identify gene loci that influence bone properties and not to examine structure-function relationships.

We sought to investigate structure-function relationships of multiple bones from a large population of genetically diverse mice of both sexes. Accordingly, we analyzed data from the femur and radius of male and female mice from the F34 generation of the Large-by-Small advanced intercross line (LG,SM AI), which have over a two-fold continuous spread of bone sizes (Silva et al., 2019). We utilized this F34 LG,SM AI population of mice in a previous study and reported the effects of diet, sex, and body mass on cortical bone traits evaluated by microCT and mechanical testing of >2200 bones. In brief, we showed female and male mice raised on a high-fat diet had increased body weight and developed larger, stronger bones compared to mice fed a low-fat diet (Silva et al., 2019).

One challenge with any in-depth phenotyping study is the volume of data, which can make analysis and interpretation overwhelming. For example, for the LG,SM AI mice, we reported 25 bone traits (14 for the radius, 11 for the femur) for 1113 animals from four experimental groups. Coulombe et al. recently highlighted limitations in comparing groups based on individual bone traits (Coulombe et al., 2021a). As an alternative, they proposed principal component analysis (PCA), k-means clustering, and Support Vector Machine classification (SVM) as complimentary methods to concurrently evaluate all traits within a data set. Specifically, PCA was used to explain the variation of bone trait values within the population using a smaller number of independent variables resulting in three principal components that explain over 90 % of the population variation in ten individual traits (Coulombe et al., 2021a; Coulombe et al., 2021b). Herein, we apply some of these approaches to the LG,SM AI data set to identify a reduced set of traits that still captures the variation in morphology or mechanical properties between animals.

Mechanical properties at the whole-bone (structural) scale are dependent on bone size and material properties. Material properties of rodent bone have traditionally been estimated from mechanical tests using engineering beam theory equations (Turner and Burr, 1993). These equations assume a uniform cross-section, homogenous and isotropic material properties, and a slender test specimen. Our group and others have shown mouse bones, especially femurs, do not meet these assumptions and calculations underestimate the true values of material properties (Turner and Burr, 1993; Schriefer et al., 2005; van Lenthe et al., 2008; Silva et al., 2004). Schriefer et al. compared the measurement error of various long bones and recommended the radius as the preferred bone for three-point bend testing due to its consistently round shape and slender aspect ratio (Schriefer et al., 2005). Despite this recommendation, over 80 % of studies reporting mechanical testing in the last 10 years tested the femur and over 60 % of those testing the femur reported material properties calculated using engineering beam theory (PubMed terms: mouse, bone, mechanical testing; published since 2011). Thus, there is a need to re-examine methods used to estimate mouse bone material properties that remain in widespread use.

Our objective in this study was to mine the dataset from the LG,SM AI population (Silva et al., 2019) to investigate relationships between and within bone traits in a mouse population with a large variation of body size and bone size. Specifically, we asked four questions: 1) What are a reduced set of traits that can describe the morphology and mechanical properties of mouse long bones? 2) Do traits correlate between long bones? 3) Can the reduced set of morphology traits accurately predict whole-bone strength? and 4) What are the implications of using beam theory to estimate material properties in the femur compared to the radius?

## 2. Methods and materials

### 2.1. Mice

All mouse work was completed with approval of the Washington University Institutional Care and Use Committee (IACUC). Data analyzed herein were previously published (Silva et al., 2019). Briefly, long bones from 1139 mice from the F34 generation of the LG/J by SM/J AI line (Wustl:LG,SM-G34) were analyzed. Males and females were divided into two diet groups and fed either a relatively high-fat (42 % calories from fat) or low-fat (15 % calories from fat) diet beginning at weaning (3 wk. of age). This resulted in four experimental groups: FL (female low-fat), FH (female high-fat), ML (male low-fat), and MH (male high-fat). Mice were euthanized at skeletal maturity (avg 24.7 wks, range = 21.0–28.7 wks). Female and male mice raised on a high-fat diet had 32 % greater body mass, on average, than sex-matched mice fed a low-fat diet. Body mass was 17 % greater in males than females (Silva et al., 2019).

### 2.2. Phenotyping

Femur and radius cortical bone phenotyping was completed as described (Silva et al., 2019). Briefly, bone cross-sectional morphology was assessed with microCT spanning a 3 mm region of the mid-diaphysis (16 μm voxel size). Bone length was measured using calipers. Whole-bone mechanical properties were assessed using three-point bending with a support span of 7 mm. Material properties were estimated using simple beam theory equations. Fourteen properties were reported per bone: six morphology traits (five that describe the cross-section, and one

the length), five whole-bone mechanical properties, and three bone material properties (Table 1). Traits were transformed as necessary to normalize the data. Any trait that was normalized is indicated with a prefix of l (natural log transform; femur yield force), i (inverse transform; femur post-yield displacement), or s (square root transform; femur work to fracture). Any mouse exhibiting extreme values (judged to be either biologically or physically implausible) in one or more traits were excluded from analysis, leaving 1113 mice (FL: $n = 274$; FH: $n = 282$; ML: n = 274; MH: $n = 283$).

### 2.3. Analysis software

Analysis and statistical comparison was done using R or GraphPad Prism. R version 4.0.2 (2020-06-22 – "Taking Off Again") was used with RStudio (Version 1.2.5042) and the Global CRAN repository to calculate the principal component analysis and correlation matrix. GraphPad Prism (version 9) was used to perform bivariate and multivariate linear analyses.

### 2.4. Principal component analysis

Principal component analysis (PCA) was performed on four datasets: 1) femur morphology, 2) radius morphology, 3) femur mechanical properties and 4) radius mechanical properties. Initially, the four experimental groups (2 sexes × 2 diets) were analyzed separately, but no differences were found between groups (Suppl. Fig. S1) so all 1113 animals were pooled and analyzed together. Each variable was centered and scaled to have a distribution mean of 0 and standard deviation of 1 within the *prcomp* function. Because signs are arbitrarily assigned to variable weights, the weightings in dataset 2 (radius morphology) were multiplied by negative one (−1) to match the signs from dataset 1 (femur morphology). Coordinates (weightings) of each variable in each principal component dimension and the variance of each principal component were extracted from the PCA. Using the PCA analysis we identified reduced sets of morphological and mechanical traits that span the principal components and are relatively independent of each other (based on Section 2.5 - Correlation matrix below).

### 2.5. Correlation matrix

A matrix of Pearson's correlation coefficients was computed on two datasets: 1) all femoral traits and 2) all radial traits. Correlations between all traits within a single bone were computed using the *cor* function in R and visualized using the *corrplot* function. Variables were automatically hierarchically clustered into five groups using the *ward.D2* algorithm.

### 2.6. Bivariate linear analysis

Bivariate linear regression was performed to 1) compare bone traits between long bones (radius vs femur) and 2) compare elastic modulus (material property) to bone size parameters (Ma.Ar, Tt.Ar, J) per bone. For all bivariate regressions, each sex/diet group was first plotted and analyzed individually, then pooled and analyzed again. The slopes were compared between groups by calculating a two-sided *p*-value. If slopes were determined to be not significantly different ($p > 0.05$) the intercepts were also compared. This method of slope and intercept comparison is equivalent to Analysis of Covariance (ANCOVA). Additionally, the slopes for each group were compared to zero using an F-test with $p < 0.05$ for significance. To compare traits between long bones, the value of a single trait measured in the radius was plotted against the same trait measured in the femur. This resulted in 14 bivariate analyses. To compare elastic modulus to bone size, the elastic modulus of the femur was plotted against either the marrow area, total area, or polar moment of inertia of the femur. The same was repeated for the radius. This resulted in 6 bivariate analyses (3 for femur and 3 for radius).

**Table 1**
List of phenotype variables measured for both the femur and radius.

| | |
|---|---|
| Morphology traits ($n = 6$) | Length (Le), cortical area (Ct.Ar), total area (Tt.Ar), marrow area (Ma.Ar), polar moment of inertia (J), average cortical thickness (Ct.Th) |
| Mechanical properties ($n = 5$) | Ultimate force (Fu), yield force (Fy), stiffness (K), post-yield displacement (PYD), work to fracture (Wfx) |
| Estimated material properties ($n = 3$) | Ultimate stress (Su), yield stress (Sy), elastic modulus (E) |

### 2.7. Multivariate linear regression

Multivariate linear regressions were performed to estimate ultimate force of the femur and radius individually. To create the multivariable model for ultimate force, the predicted value was set to ultimate force while the independent variables were initially set to all morphology traits ($n = 6$). First, backward elimination was used to reduce the variable set to only those significantly and independently contributing to the model. Briefly, the variable with the highest *p*-value was removed from the model and the analysis was re-run until all remaining variables had a significant contribution ($p < 0.05$). A second model was created using the three morphology parameters proposed in the reduced set of parameters (Ct.Ar., Ma.Ar., Le). The best fit of each model was assessed using the adjusted $R^2$ value.

## 3. Results

### 3.1. Correlation of traits within each bone

We used principal component analysis (PCA) to examine how bone traits cluster during dimensional reduction. Dimensional reduction can allow for fewer variables to characterize the data set while maintaining the majority of the variability in the population. In both the femur and radius, bone morphometry parameters can be reduced to three components that explain almost 99 % of the variation between animals (Fig. 1). Clustering of traits is almost identical in the femur and radius. While all variables contribute, the first principal component (PC1) is dominated by the bone size parameters total area, cortical area, and moment of inertia; these three variables are highly correlated ($r > 0.79$ for each pair) and fall into the same hierarchical cluster (Fig. 3). PC2 is dominated by two additional cross-sectional parameters, marrow area and cortical thickness, which contribute to PC2 in opposite directions; these variables are not significantly correlated. Bone length is the only parameter that significantly contributes to PC3. Thus, the five measured bone traits that describe cortical cross-sectional morphology can be reduced to two principal components, while bone length adds a third component. Thus, cortical area, marrow area and length represent a reduced set of parameters that characterize long bone morphology in this mouse population.

Similarly, the five measured mechanical properties reduce to two dimensions that explain 80 % and 90 % of the variation between animals in the femur and radius, respectively (Fig. 2). PC1 is mainly defined by bone stiffness and strength. PC2 is defined by properties that reflect bone ductility (PYD and Wfx); these two properties are highly and almost exclusively correlated to each other and cluster together (Fig. 3). Thus, ultimate force and post-yield displacement represent a reduced set of parameters that characterize long bone mechanical properties.

The three estimated material properties moderately or highly correlate with each other in both the femur and radius, but this correlation is stronger in the radius (Fig. 3). Within the femur, material properties (especially elastic modulus) have negative correlations with multiple bone morphology parameters, whereas these correlations are absent in the radius.

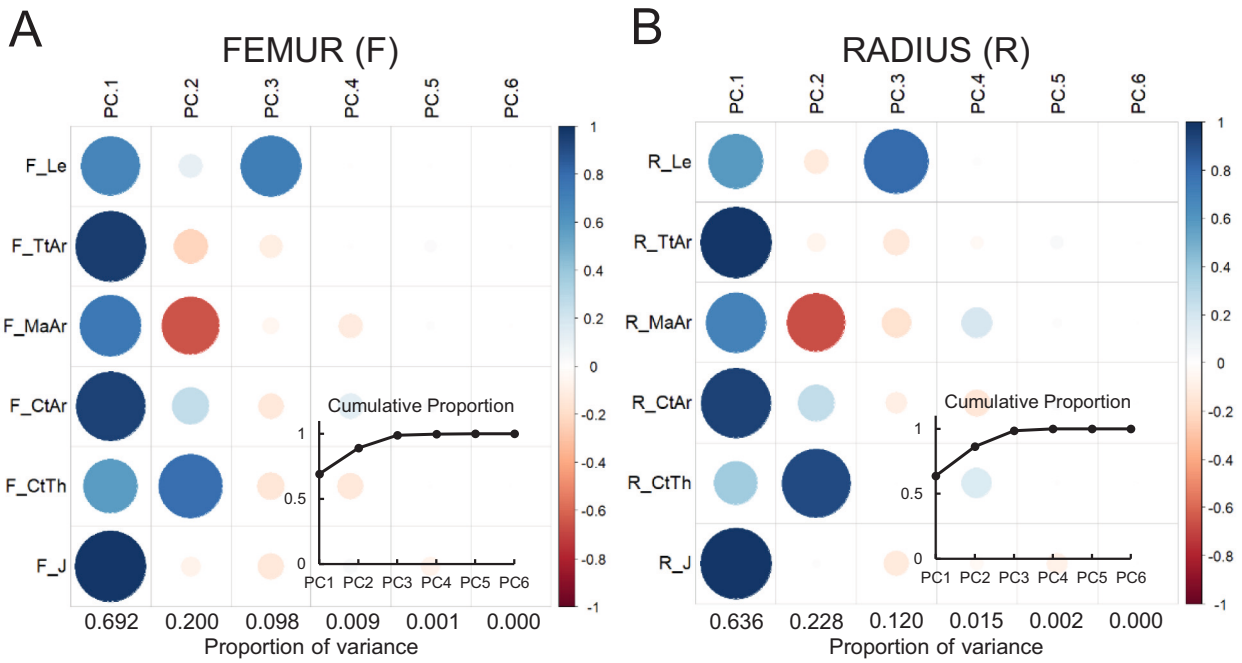


**Fig. 1.** PCA of morphology parameters in the femur and radius.
Contribution of each morphology parameter collected from uCT of the femur (A) and radius (B) to the individual dimensions of a principal component analysis (PCA). For both bones, the first three components (PC) explain over 90 % of variation between animals. TtAr, CtAr, and J contribute the most to PC1. MaAr and CtTh contribute the most to PC2. Le is the only variable highly contributing to PC3. Inset graphs show cumulative proportion of variance from each principal component.
F: femur, R: radius, Le: length, TtAr: total area, MaAr: marrow area, CtAr: cortical area, CtTh: cortical thickness, J: moment of inertia, PC: principal component.

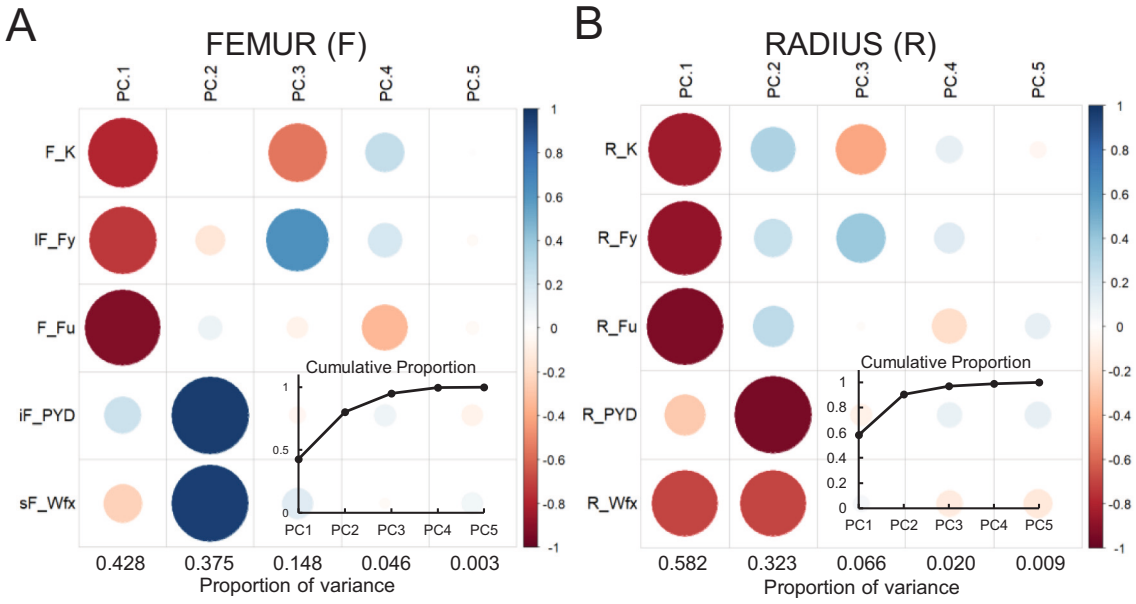


**Fig. 2.** PCA of mechanical properties in the femur and radius.
Contributions of each mechanical property collected from 3 pt. bending of the femur (A) and radius (B) to the individual dimensions of a principal component analysis (PCA). For the femur, the first two components (PC) explain over 80 % of variation between animals. For the radius, the first two components explain over 90 % of variation between animals. K, Fy, and Fu (stiffness and strength properties) contribute the most to PC1. PYD and Wfx (ductility properties) contribute the most to PC2. Inset graphs show cumulative proportion of variance from each principal component.
F: femur, R: radius, Fu: ultimate force, Fy: yield force, K: stiffness, PYD: post-yield displacement, Wfx: work to fracture, PC: principal component.

### *3.2. Correlation of traits between bones*

We used bivariate linear regression to investigate how each trait correlates between two long bones, the femur and radius. All morphology traits are positively and significantly correlated between bones. Notably, the relationships between bones do not depend on sex or diet (i.e., slopes of regression lines are not different between groups; Fig. 4). We note that there are significant differences in intercepts between groups, but intercepts from the pooled data are within the 95 % confidence interval of the intercept for each group. The $R^2$ values for

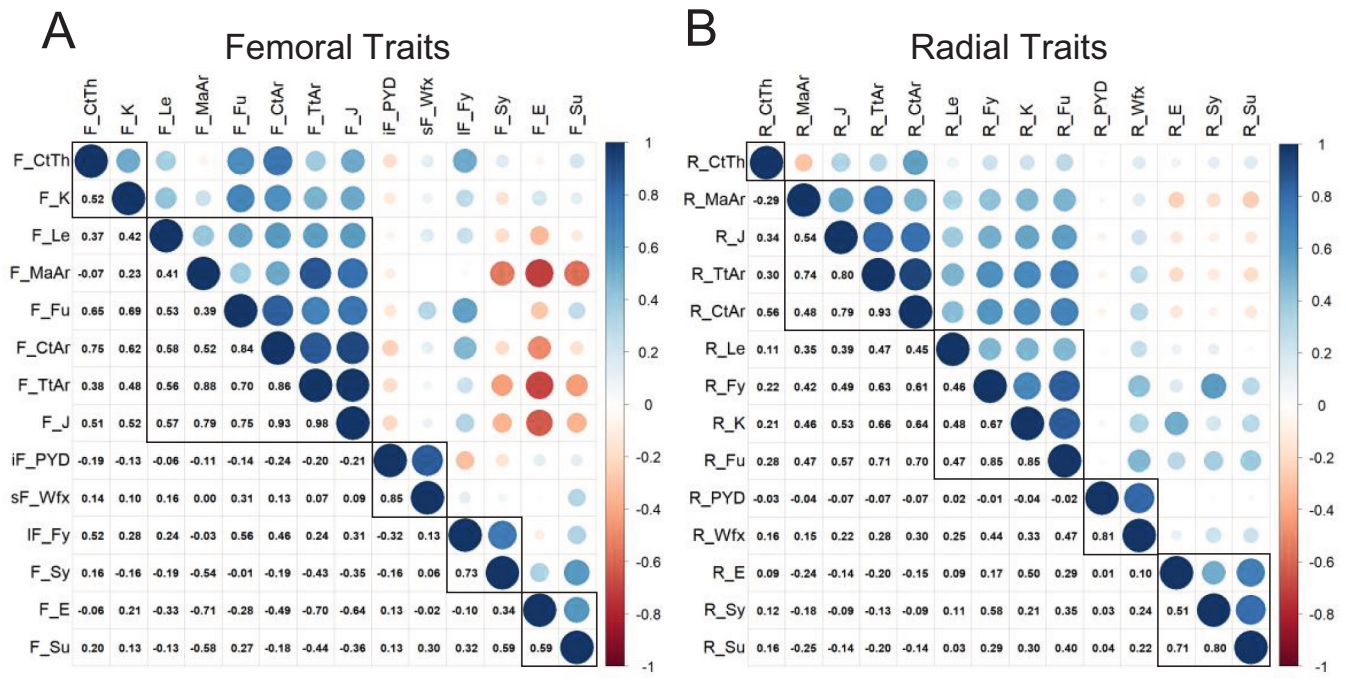


**Fig. 3.** Pearson's correlation matrix for all measured bone traits in the femur and radius.
Correlation matrix of all 14 bone properties measured for the femur (A) and radius (B). Black boxes surround variables that cluster together using hierarchical clustering. Material properties (Sy, Su, E) highly correlate with each other for both bones. E in the femur has negative correlation with many morphometry parameters, a relationship absent in the radius. Lower triangle shows Pearson's r values.
F: femur, R: radius, Le: length, TtAr: total area, MaAr: marrow area, CtAr: cortical area, CtTh: cortical thickness, J: moment of inertia, Fu: ultimate force, Fy: yield force, K: stiffness, PYD: post-yield displacement, Wfx: work to fracture, Su: ultimate stress, Sy: yield stress, E: elastic modulus.

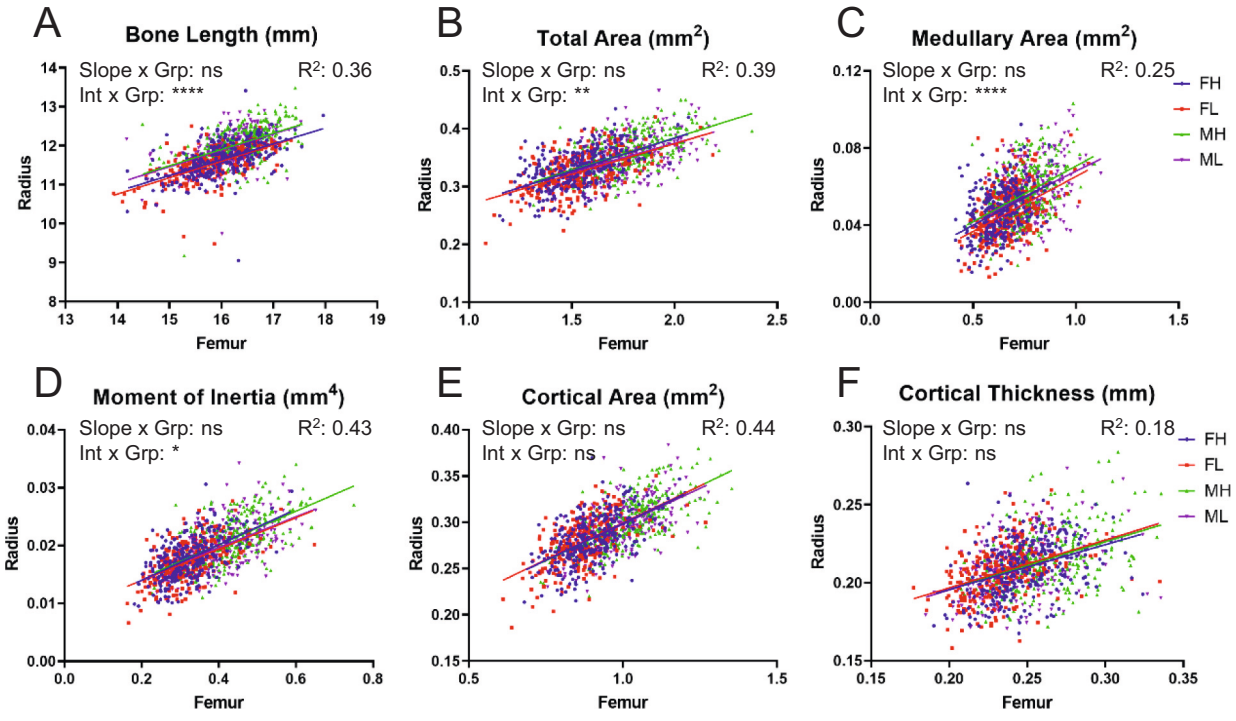


**Fig. 4.** Morphology correlations between femur and radius.
Correlation of morphology traits between the femur (x-axis) and radius (y-axis) with linear regression lines displayed per sex/diet group. Slopes are not significantly different between sex/diet groups, for any variable. Intercept values are significantly different for bone length (A), total area (B), medullary area (C), and moment of inertia (D). For all traits and all groups, the slopes of the linear regression line are significantly different from zero. Goodness of fit ($R^2$) for all groups pooled is shown on each graph.
Slope: significance of different slopes between groups, Int: significance of different intercepts between groups, ns: not significant, *$p < 0.05$, **$p < 0.01$, ***$p < 0.001$, ****$p < 0.0001$, FH: female high fat, FL: female low fat, MH: male high fat, ML: male low fat.

each sex-diet group are generally similar, which is further indication that there is a similar relationship between bones across the four groups (Supp. Table S1). When sex/diet groups are pooled, cortical area and moment of inertia have the strongest correlations between bones ($R^2$ = 0.44 and 0.43, respectively; Fig. 4), while medullary area and cortical thickness have the weakest correlations ($R^2$ = 0.25 and 0.18, respectively; Fig. 4). Thus, morphological traits related to size of the radius and femur are moderately well correlated in this mouse population and these relationships are similar across sex and diet.

Mechanical properties are weakly correlated between long bones (Fig. 5). Ultimate force is the only mechanical property where the slopes are different between sex/diet groups ($p$ = 0.03); individual group slopes range from 32 % lower to 12 % higher than the pooled slope (Supp. Table S2). For post-yield displacement, all four sex/diet groups have slopes not different from zero indicating no correlation between the femur and radius. Additionally, despite having no significant differences in slopes between groups, only female low-fat (FL) and male high-fat (MH) have slopes not different from zero for work-to-fracture. Material properties are not correlated between long bones, where all four sex/diet groups for the three material properties have slopes not significantly different from zero (Fig. 6). The estimated values for each material property are approximately two times higher in the radius than the femur. Thus, whole-bone mechanical properties of the radius and femur are only weakly correlated, while estimated material properties are not correlated.

### 3.3. Prediction of whole-bone strength

We created a multivariate linear regression to predict ultimate force, a measure of whole-bone strength, from morphology parameters (Fig. 7). Ultimate force can be predicted with moderate accuracy for both bones, with the femur prediction being more accurate (adj $R^2$ = 0.72 (fem) vs. 0.54 (rad)) (Fig. 7.A, B). After using backwards elimination to exclude non-significant contributing variables, the femur ultimate force can be well predicted from cortical area, moment of inertia, cortical thickness, and length (Fig. 7.A). Note that these four parameters span the three main PCs explaining a majority of the intra-bone variation (Fig. 1.A). For the radius, only total area, marrow area, and length are needed to predict ultimate force (Fig. 7.B), which corresponds to one variable per PC cluster (Fig. 1.B). For both bones, the largest contributing variable is a measure of cross-sectional bone size. We compared this non-biased model to a model using a pre-selected reduced set of morphology traits (Ct.Ar, Ma.Ar, Le; determined in Section 3.1 - Correlation of traits within each bone). The goodness of fit is almost identical to that of the un-biased model (adj $R^2$ = 0.71 (fem) and 0.54 (rad); Fig. 7.C, D) supporting the finding that these three parameters are a functionally meaningful set.

### 3.4. Implications of using beam theory to predict material properties

Finally, we further examined the negative correlations between material properties and morphology parameters identified in the correlation matrix (Fig. 3). In the femur, elastic modulus correlated strongly with marrow area, total area, and moment of inertia ($r$ = −0.64 to −0.71; $p < 0.0001$). These same correlations in the radius were much weaker, albeit significant ($r$ = −0.16 to −0.25; $p < 0.0001$). We used bivariate linear regression to investigate these relationships individually (Fig. 8). Marrow area correlates the most strongly to elastic modulus and this correlation is much stronger in the femur than radius ($R^2$ = 0.51, fem (Fig. 8.A) vs 0.061, rad (Fig. 8.D)). Total area correlates moderately

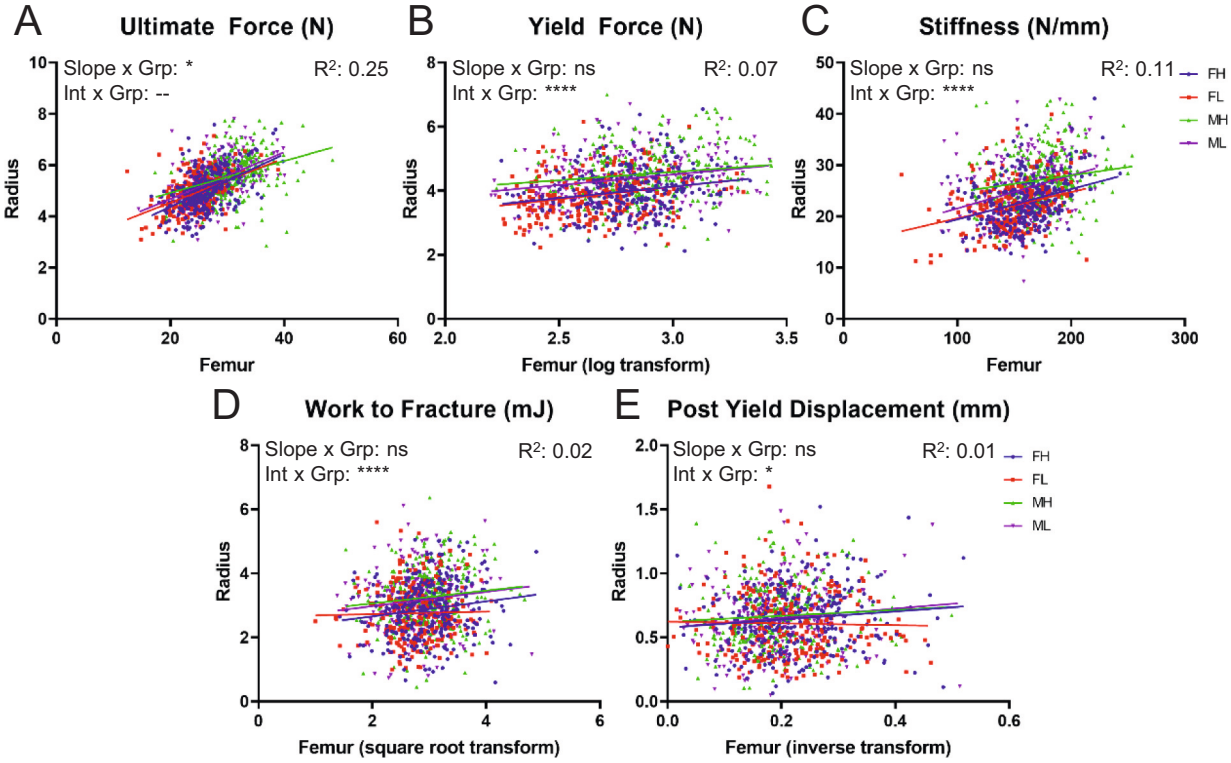


**Fig. 5.** Mechanical property correlations between femur and radius.
Correlation of mechanical properties between the femur (x-axis) and radius (y-axis) with linear regression lines displayed per sex/diet group. Slopes are not significantly different between sex/diet groups, except for ultimate force (A). Intercept values are significantly different for all other traits (B-E). For ultimate force (A), yield force (B), and stiffness (C), the slopes of the linear regression line are significantly different from zero. For work to fracture, best fit lines from the FL and MH groups are not significantly different from zero. The post-yield displacement regression lines are not significantly different from zero for all sex/diet groups.
Slope: significance of different slopes between groups, Int: significance of different intercepts between groups, ns: not significant, –: not evaluated, *$p < 0.05$, **$p < 0.01$, ***$p < 0.001$, ****$p < 0.0001$, FH: female high fat, FL: female low fat, MH: male high fat, ML: male low fat.

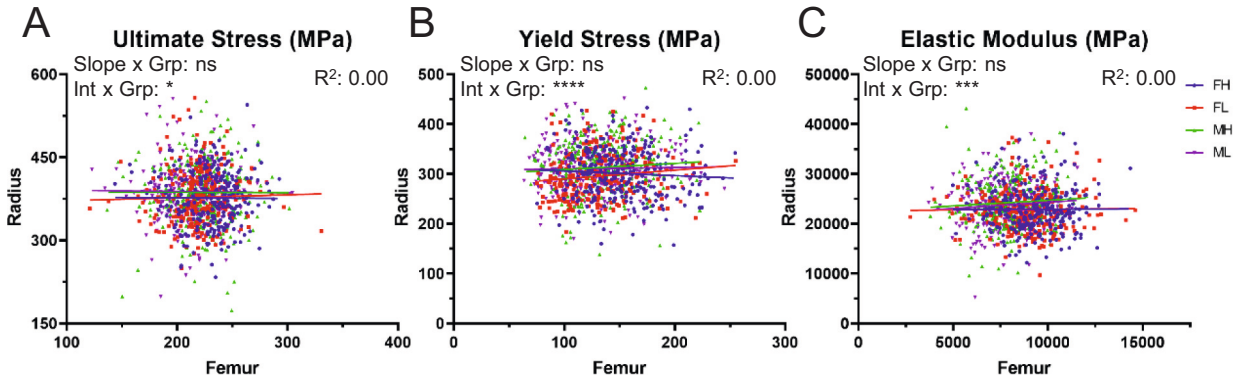


**Fig. 6.** Material property correlations between femur and radius.
Correlation of material properties between the femur (x-axis) and radius (y-axis) with linear regression lines displayed per sex/diet group. The slopes of the linear regression line are not significantly different from zero for any material property trait, and are not significantly different between sex/diet groups. Intercept values are significantly different for all traits (A–C).
Slope: significance of different slopes between groups, Int: significance of different intercepts between groups, ns: not significant, *p < 0.05, **p < 0.01, ***p < 0.001, ****p < 0.0001, FH: female high fat, FL: female low fat, MH: male high fat, ML: male low fat.

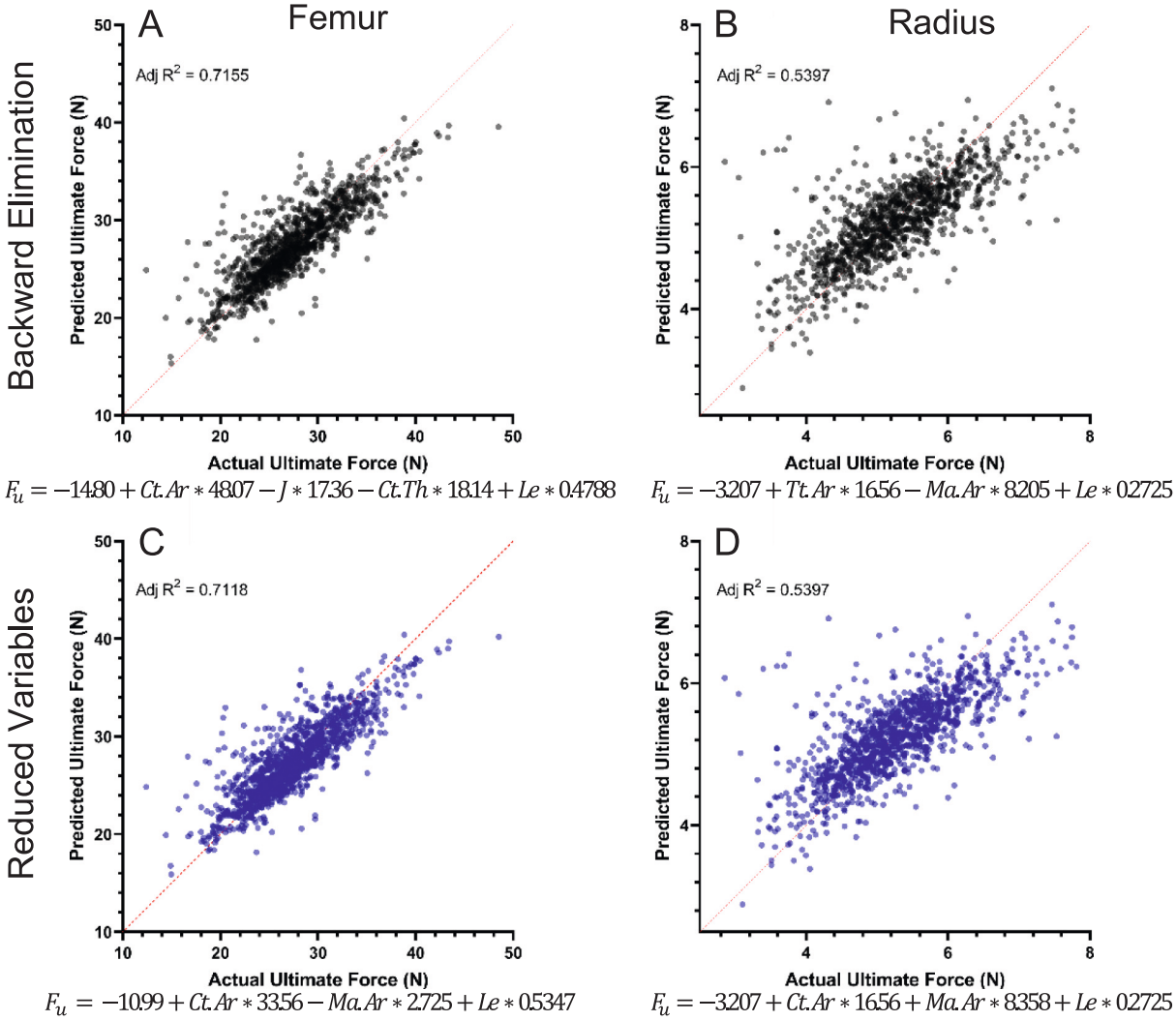


**Fig. 7.** Prediction of ultimate force.
Multivariate linear regression of ultimate force for the femur (A & C) and radius (B&D). (A & B) All morphology parameters were initially included in the model. Backwards elimination was used to narrow down only significantly contributing variables. (C & D) Only the reduced set of morphology parameters (Ct.Ar, Ma.Ar, Le) were included in the model. The $R^2$ value is extremely similar between models within each bone. Ultimate force is more accurately predicted in the femur compared to the radius, as shown by the larger adjusted $R^2$ value.

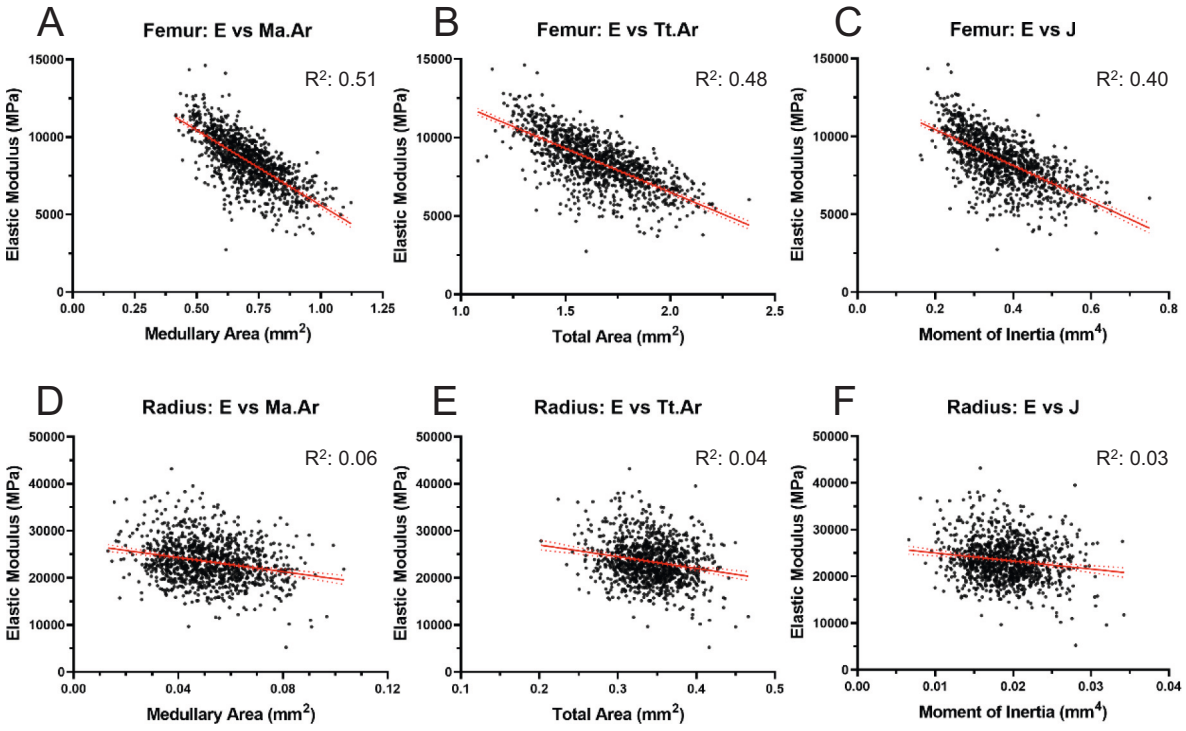


**Fig. 8.** Correlation of elastic modulus with morphology parameters.
Correlation of elastic modulus with morphology parameters in the femur (A–C) and radius (D–F). Medullary area correlates most strongly with elastic modulus for both bones (A & D), but the correlation is stronger in the femur. For each trait, the correlation is stronger in the femur (top row) compared to the radius (bottom row). All slopes from the linear regression are significantly different from zero. All 4 sex/diet groups were combined for analysis.

to elastic modulus in the femur (Fig. 8.B) yet very weakly in the radius (Fig. 8.E). Moment of inertia had the weakest correlation to elastic modulus, but was still moderately correlated in the femur ($R^2 = 0.40$; Fig. 8.C). The radius shows a very weak correlation between elastic modulus and moment of inertia ($R^2 = 0.025$; Fig. 8.F). Taken together, these analyses indicate that beam theory-estimated material properties for the femur have a strong dependence on morphology, while the estimated material properties of the radius have only a weak dependence on morphology.

## 4. Discussion

We reported previously that long bone traits are different between sexes and are altered by diet in LG,SM AI mice (Silva et al., 2019). Using these same data from >1100 mice, here we focused on the intra- and inter-bone relationships to address four questions: 1) What are a reduced set of traits that can describe the morphology and mechanical properties of mouse long bones? 2) Do traits correlate between bones? 3) Can the reduced set of morphology traits accurately predict bone strength? and 4) What are the implications of using beam theory to estimate material properties in the femur compared to the radius? We find that PCA and correlation analysis reveals similar relationships between morphological and mechanical properties across the sex/diet groups for both the femur and radius, which implies that relationships between bone parameters were conserved across sex, diet, and bone. This suggests that the reduced set of parameters we report here may be useful to describe mouse long bones from other populations. Correlations of individual traits between long bones reveal that morphology parameters are positively and strongly correlated, whereas mechanical and material properties have weak to no correlations between bones. These correlations are again independent of sex or diet. Multivariate regression reveals that 54–72 % of variation in ultimate force can be predicted from bone morphology measured using microCT. Finally, elastic modulus and bone morphology are moderately correlated for the femur but not the radius. The dependency of material property estimates in the femur on morphology raises the possibility of a size-dependent error when using beam theory to estimate material properties of mouse femurs.

We investigated *intra*-bone relationships of cortical bone traits using principal component analysis (PCA) to evaluate which combination of variables contribute the most to bone variability in the F34 LGXSM AI population. Reducing dimensionality using PCA can simplify interpretation while minimizing data loss. Additionally, we built a correlation matrix to investigate the relationship of each pair of traits. Using these analyses, we identified a minimal set of cortical bone properties (traits) to describe mouse long bones that may be useful when assessing differences between experimental groups or variations within other mouse populations. For morphometry we identified *cortical area*, *medullary area*, and *bone length*; these parameters span the first three principal components and together can describe bone expansion periosteally, endosteally, and axially. For mechanical properties we identified *ultimate force* and *post-yield displacement*; these two parameters are independent, contribute almost exclusively to different principal components, and represent a force measurement and deformation measurement. Compared to other measurements that describe whole-bone function (e.g., stiffness), ultimate force is more accurately computed since it is independent of deformation measurements, and ultimate force had the strongest correlations to morphology parameters in our data set (Fig. 3). For material properties, we identify *ultimate stress*. Calculations of ultimate stress do not depend on strain estimation and are therefore less variable and more accurate than modulus estimations (Jepsen et al., 2015).

We investigated *inter*-bone relationships between the femur and radius using bivariate linear regressions for each of the fourteen traits reported. Morphometry traits are all significantly and positively correlated between long bones. The lack of significant difference in slopes between the sex/diet groups in all these correlations indicates that morphometry traits scale between long bones independently of sex or diet. In contrast to the moderately strong correlations between bones for

morphometric properties, mechanical properties are only weakly correlated. Ultimate force is the most strongly correlated ($R^2 = 0.25$) between the radius and femur, followed by bone stiffness ($R^2 = 0.11$). The correlation between radius and femur for ultimate force reported here for mice is comparable to the correlation reported in Patton et al. for humans (Patton et al., 2019). However, work-to-fracture and post yield displacement do not correlate between long bones indicating yielding behavior and ductility assessed by three-point bending are bone-dependent properties. Estimated material properties have no correlation between long bones. While this result could mean that murine bone material properties differ between bones, it may be an artifact of inaccurate estimations of femur material properties using beam theory. To answer this question, more direct methods to estimate material properties are required. Regardless, the lack of strong correlation of mechanical and material properties between the radius and femur indicates that the results from routine three-point bending tests of one long bone (e.g., femur) may not be generalizable to another long bone (e.g., radius).

Next, we investigated the feasibility of predicting bone strength using bone morphology determined by microCT. If variation in bone strength can be estimated using non-destructively measured parameters, physically breaking bones may be unnecessary and bone samples could be used for other outcomes (e.g., histology). The unbiased multi-variable model we report here can predict nearly 72 % of the variation in ultimate force in the femur and nearly 54 % in the radius. A reduced set of morphology parameters predict the same amount of variation as the unbiased model for both bones. Additionally, using just one of the morphometry parameters in the reduced set (cortical area) explains nearly the same amount of variation in ultimate force (71 % for femur, 49 % for radius). Bone mineral density alone can explain 50–75 % of the variation in ultimate strength in various mammalian models, and around 57 % for rat humerus (Ammann and Rizzoli, 2003), which is similar to the range of variation explained by our model. Additionally, other groups have used similar multivariable models and have been able to predict almost 80 % of femur strength using bone volume, cortical thickness, and total area (Voide et al., 2008). The higher goodness of fit of the model in that study might be due to the differences in mouse number, range of bone sizes, and measurement technique. While morphometry-based estimation of bone strength is an appealing concept, 28–46 % of variation in ultimate force was not explained by our model leading us to conclude that mechanical testing is still essential to assess differences in bone strength between experimental groups.

Finally, we investigated the implications of using beam theory to estimate bone material properties. Three- (or four-) point bending is the preferred method to mechanically test bones of small animals (Jepsen et al., 2015). Typically, material properties are estimated using engineering beam theory where the test specimen is assumed to have a constant cross-section, homogenous and isotropic properties, and a large length-to-width ratio. The femur, which is the most common bone used for mechanical testing, does not meet these assumptions and therefore estimated values of material properties are generally underestimated (Jepsen et al., 2015; Schriefer et al., 2005; van Lenthe et al., 2008). The radius is a longer, more slender bone that more accurately meets beam theory assumptions, but can be more difficult to handle and requires more sensitive testing equipment due to its small size. A previous study comparing the accuracy between the radius and femur did so in mouse bones of two genetic backgrounds having distinctly different bone size (B6, C3H) (Schriefer et al., 2005). The mice in the current study have a more continuous range of bone sizes and strengths and include larger variations of genetic backgrounds, allowing us to test if the limitations of applying beam theory to mouse bones are more broadly applicable. We found strong correlations of elastic modulus with bone morphometry parameters in the femur only, with 40–50 % of variation in elastic modulus being explained by bone geometry. These correlations are almost entirely absent in the radius, with only 2.5–6 % of the variation in elastic modulus being explained by bone geometry. This suggests that size differences in bones may bias femur-estimated values of material properties much more so than radius-estimated properties. These findings provide additional support to previous recommendations for mechanical testing of the radius when a goal is to estimate material properties (Jepsen et al., 2015; Schriefer et al., 2005).

In summary, we used a large, previously published data set (Silva et al., 2019) from mice spanning a large range of body size and weight to investigate the structure-function relationship of two long bones and the dependency on sex and diet. In both the femur and radius, bone traits similarly cluster together using PCA and correlation analysis. Additionally, how bone traits cluster did not change based on sex/diet groups. The independence on bone type, sex, and diet provide support that these correlations are more broadly applicable to cortical traits of long bones from various mouse populations. We identified a reduced set of parameters for morphometry, mechanical properties, and material properties that are fairly independent yet span the various principal components to explain the most variation in the population. For morphometry, we identified cortical area, medullary area, and bone length; for mechanical properties, we identified ultimate force and post-yield displacement; for material properties, we identified ultimate stress. We observed that up to 50 % of the variation in femur-estimated elastic modulus could be explained by size parameters, which suggests that caution should be taken when interpreting estimated material properties of the femur. Finally, while many morphometry parameters are highly correlated with mechanical properties, predicting ultimate force from morphometry alone did not account for up to 50 % of the variation between animals in our study, highlighting the value of destructive mechanical testing. Our results support that testing be done on the bone of interest because mechanical, and especially material, properties correlated poorly between the femur and radius.

Supplementary data to this article can be found online at https://doi.org/10.1016/j.bonr.2022.101615.

## CRediT authorship contribution statement

**Nicole Migotsky:** Conceptualization, Methodology, Software, Formal analysis, Writing – original draft, Writing – review & editing, Visualization. **Michael D. Brodt:** Investigation, Writing – review & editing. **James M. Cheverud:** Writing – review & editing, Funding acquisition. **Matthew J. Silva:** Conceptualization, Writing – review & editing, Supervision, Funding acquisition.

## Declaration of competing interest

The authors declare the following financial interests/personal relationships which may be considered as potential competing interests:

Nicole Migotsky: None

Michael D. Brodt: None

James M. Cheverud: None

Matthew J. Silva COI: Editorial Board Bone, Calcified Tissue International, Journal of Orthopaedic Research

## Acknowledgements

We would like to acknowledge our funding sources from the National Institutes of Health (P30 AR074992/NIAMS NIH, R01 AR047867/NIAMS NIH, R01 DK075112/NIDDK NIH).

## References

Ammann, P., Rizzoli, R., 2003. Bone strength and its determinants. Osteoporos. Int. 14 (3), 13–18. https://doi.org/10.1007/S00198-002-1345-4.

Berman, A.G., Clauser, C.A., Wunderlin, C., Hammond, M.A., Wallace, J.M., 2015. Structural and mechanical improvements to bone are strain dependent with axial compression of the tibia in female C57BL/6 mice. PLoS One 10 (6), 1–16. https://doi.org/10.1371/journal.pone.0130504.

Bonadio, J., Jepsen, K.J., Mansoura, M.K., Jaenisch, R., Kuhn, J.L., Goldstein, S.A., 1993. A murine skeletal adaptation that significantly increases cortical bone mechanical properties. Implications for human skeletal fragility. J. Clin. Invest. 92 (4), 1697–1705. https://doi.org/10.1172/JCI116756.

Brent, M.B., Stoltenborg, F.E., Brüel, A., Thomsen, J.S., 2021. Teriparatide and abaloparatide have a similar effect on bone in mice. Front. Endocrinol. (Lausanne). 12 (April), 1–9. https://doi.org/10.3389/fendo.2021.628994 (Lausanne).

Brodt, M.D., Ellis, C.B., Silva, M.J., 1999. Growing C57Bl/6 mice increase whole bone mechanical properties by increasing geometric and material properties. J. Bone Miner. Res. 14 (12), 2159–2166. https://doi.org/10.1359/JBMR.1999.14.12.2159.

Burstein, A.H., Frankel, V.H., 1971. A standard test for laboratory animal bone. J. Biomech. 4 (2), 155–158. https://doi.org/10.1016/0021-9290(71)90026-1.

Cole, J.H., van der Meulen, M.C.H., 2011. Whole bone mechanics and bone quality. Clin. Orthop. Relat. Res. 469 (8), 2139. https://doi.org/10.1007/S11999-011-1784-3.

Coulombe, J.C., Mullen, Z.K., Lynch, M.E., Stodieck, L.S., Ferguson, V.L., 2021. Application of machine learning classifiers for microcomputed tomography data assessment of mouse bone microarchitecture. MethodsX 8, 101497. https://doi.org/10.1016/j.mex.2021.101497.

Coulombe, J.C., Sarazin, B.A., Mullen, Z., et al., 2021. Microgravity-induced alterations of mouse bones are compartment- and site-specific and vary with age. Bone 151, 116021. https://doi.org/10.1016/J.BONE.2021.116021.

Gardinier, J.D., Al-Omaishi, S., Morris, M.D., Kohn, D.H., 2016. PTH signaling mediates perilacunar remodeling during exercise. Matrix Biol. 52–54, 162–175. https://doi.org/10.1016/J.MATBIO.2016.02.010.

Goodship, A.E., Lanyon, L.E., McFie, H., 1979. Functional adaptation of bone to increased stress. J. Bone Jt. Surg. 61-A (4), 539–546.

N Holguin MD Brodt ME Sanchez AA Kotiya MJ Silva. Adaptation of Tibial Structure and Strength to Axial Compression Depends on Loading-History in Both C57BL/6 and BALB/C Mice. doi:10.1007/s00223-013-9744-4.

Jepsen, K.J., Pennington, D.E., Lee, Y.-L., Warman, M., Nadeau, J., 2001. Bone brittleness varies with genetic background in A/J and C57BL/6J inbred mice. J. Bone Miner. Res. 16 (10), 1854–1862. https://doi.org/10.1359/JBMR.2001.16.10.1854.

Jepsen, K.J., Akkus, O., Majeska, R.J., Nadeau, J.H., 2003. Hierarchical relationship between bone traits and mechanical properties in inbred mice. Mamm. Genome 14 (2), 97–104. https://doi.org/10.1007/s00335-002-3045-y.

Jepsen, K.J., Akkus, O.J., Majeska, R.J., Nadeau, J.H., 2003. Hierarchical relationship between bone traits and mechanical properties in inbred mice. Mamm. Genome 14 (2), 97–104. https://doi.org/10.1007/S00335-002-3045-Y.

Jepsen, K.J., Silva, M.J., Vashishth, D., Guo, X.E., Van Der Meulen, M.C.H., 2015. Establishing biomechanical mechanisms in mouse models: practical guidelines for systematically evaluating phenotypic changes in the diaphyses of long bones. J. Bone Miner. Res. 30 (6), 951–966. https://doi.org/10.1002/jbmr.2539.

Lang, D.H., Sharkey, N.A., Mack, H.A., et al., 2005. Quantitative trait loci analysis of structural and material skeletal phenotypes in C57BL/6J and DBA/2 second-generation and recombinant inbred mice. J. Bone Miner. Res. 20 (1), 88–99. https://doi.org/10.1359/JBMR.041001.

Lanyon, L.E., Goodship, A.E., Pye, C.J., MacFie, J.H., 1982. Mechanically adaptive bone remodelling. J. Biomech. 15 (3), 141–154. https://doi.org/10.1016/0021-9290(82)90246-9.

Mikić, B., Van Der Meulen, M.C.H., Kingsley, D.M., Carter, D.R., 1995. Long bone geometry and strength in adult BMP-5 deficient mice. Bone 16 (4), 445–454. https://doi.org/10.1016/8756-3282(95)90190-6.

Mikić, B., Van Der Meulen, M.C.H., Kingsley, D.M., Carter, D.R., 1996. Mechanical and geometric changes in the growing femora of BMP-5 deficient mice. Bone 18 (6), 601–607. https://doi.org/10.1016/8756-3282(96)00073-7.

Patton, D.M., Bigelow, E.M.R., Schlecht, S.H., Kohn, D.H., Bredbenner, T.L., Jepsen, K.J., 2019. The relationship between whole bone stiffness and strength is age and sex dependent. J. Biomech. 83, 125–133. https://doi.org/10.1016/j.jbiomech.2018.11.030.

Pelker, R.R., Friedlaender, G.E., Markham, T.C., Panjabi, M.M., Moen, C.J., 1983. Effects of freezing and freeze-drying on the biomechanical properties of rat bone. J. Orthop. Res. 1 (4), 405–411. https://doi.org/10.1002/jor.1100010409.

Schriefer, J.L., Robling, A.G., Warden, S.J., Fournier, A.J., Mason, J.J., Turner, C.H., 2005. A comparison of mechanical properties derived from multiple skeletal sites in mice. J. Biomech. 38 (3), 467–475. https://doi.org/10.1016/j.jbiomech.2004.04.020.

Silva, M.J., Brodt, M.D., Fan, Z., Rho, J.Y., 2004. Nanoindentation and whole-bone bending estimates of material properties in bones from the senescence accelerated mouse SAMP6. J. Biomech. 37 (11), 1639–1646. https://doi.org/10.1016/j.jbiomech.2004.02.018.

Silva, M.J., Eekhoff, J.D., Patel, T., et al., 2019. Effects of high-fat diet and body mass on bone morphology and mechanical properties in 1100 advanced intercross mice. J. Bone Miner. Res. 34 (4), 711–725. https://doi.org/10.1002/jbmr.3648.

Turner, C.H., Burr, D.B., 1993. Basic biomechanical measurements of bone: a tutorial. Bone 14 (4), 595–608. https://doi.org/10.1016/8756-3282(93)90081-K.

Turner, C.H., Sun, Q., Schriefer, J., et al., 2003. Congenic mice reveal sex-specific genetic regulation of femoral structure and strength. Calcif. Tissue Int. 73 (3), 297–303. https://doi.org/10.1007/s00223-002-1062-1.

van Lenthe, G.H., Voide, R., Boyd, S.K., Müller, R., 2008. Tissue modulus calculated from beam theory is biased by bone size and geometry: implications for the use of three-point bending tests to determine bone tissue modulus. Bone 43 (4), 717–723. https://doi.org/10.1016/j.bone.2008.06.008.

Voide, R., van Lenthe, G.H., Müller, R., 2008. Bone morphometry strongly predicts cortical bone stiffness and strength, but not toughness, in inbred mouse models of high and low bone mass. J. Bone Miner. Res. 23 (8), 1194–1203. https://doi.org/10.1359/JBMR.080311.